Geomorphology xxx (2014) xxx–xxx

Contents lists available at ScienceDirect

Geomorphology

journal homepage: www.elsevier.com/locate/geomorph

Multi-spatial analysis of aeolian dune-field patterns

Ryan C. Ewing [a,*], George D. McDonald [b], Alex G. Hayes [b]

[a] Department of Geology and Geophysics, Texas A&M University, College Station, TX 77840, USA
[b] Department of Astronomy, Cornell University, Ithaca, NY 14853, USA

ARTICLE INFO

Article history:
Received 7 May 2014
Received in revised form 18 November 2014
Accepted 25 November 2014
Available online xxxx

Keywords:
Sand dunes
Dune-field patterns
Bedforms
Aeolian
Mars
Titan

ABSTRACT

Aeolian dune-fields are composed of different spatial scales of bedform patterns that respond to changes in environmental boundary conditions over a wide range of time scales. This study examines how variations in spatial scales of dune and ripple patterns found within dune fields are used in environmental reconstructions on Earth, Mars and Titan. Within a single bedform type, different spatial scales of bedforms emerge as a pattern evolves from an initial state into a well-organized pattern, such as with the transition from protodunes to dunes. Additionally, different types of bedforms, such as ripples, coarse-grained ripples and dunes, coexist at different spatial scales within a dune-field. Analysis of dune-field patterns at the intersection of different scales and types of bedforms at different stages of development provides a more comprehensive record of sediment supply and wind regime than analysis of a single scale and type of bedform. Interpretations of environmental conditions from any scale of bedform, however, are limited to environmental signals associated with the response time of that bedform. Large-scale dune-field patterns integrate signals over long-term climate cycles and reveal little about short-term variations in wind or sediment supply. Wind ripples respond instantly to changing conditions, but reveal little about longer-term variations in wind or sediment supply. Recognizing the response time scales across different spatial scales of bedforms maximizes environmental interpretations from dune-field patterns.

1. Introduction

The striking similarity of aeolian dune-field patterns across Earth, Mars, Venus and Titan demonstrates that self-organization within the complex system of sediment transport gives rise to similar patterns independent of differences in gravity, atmospheric pressure and type of sediment. The well-organized patterns created by dune fields are defined by regular spacing and crestline orientation and provide a means to recognize sand dunes on planetary surfaces. The presence of sand dunes, in turn, implies the production of a sediment size fraction capable of being transported by wind and the presence of surface winds that at some time were capable of transporting sediment (Greeley and Iversen, 1985; Kocurek and Ewing, 2012). Determining specific environmental signals such as wind direction, grain size, sediment supply and source area from well-organized dune-field patterns, however, has proven difficult because these signals are integrated into the organization of the pattern (Rubin and Hunter, 1987).

Approaches to extracting environmental signals from bedform patterns include mapping and measurement of ripple and dune patterns from aerial and satellite imagery (Mabbutt and Wooding, 1983; Fenton et al., 2003; Ewing et al., 2010; Bullard et al., 2011; Silvestro et al., 2013); laboratory and field experiments (Rubin and Hunter, 1987; Rubin and Ikeda, 1990; Kocurek et al., 1992; Reffet et al., 2010; Ping et al., 2014); and computer simulations (Werner, 1995; Bishop et al., 2002; Parteli et al., 2009; Zhang et al., 2010). This range of approaches, paired with increased availability of high spatial- and temporal-resolution data, has highlighted that environmental interpretations from dune-field patterns are maximized by studying variability in dune fields defined by the intersection of different spatial scales of bedforms that coexist within a dune field (Warren and Kay, 1987; Werner, 2003; Ewing and Kocurek, 2010; Bridges et al., 2012; Ayoub et al., 2014; Murray et al., 2014).

This paper examines a range of bedform patterns and processes that coexist in dune fields and that can be used to interpret environmental and climatic conditions within the context of dune-field pattern formation (Werner, 1999). Examples of bedform patterns are shown for Earth, Mars and Titan. The conclusion reached by this paper is that the composite pattern of dunes and ripples in a dune field is dictated by the stage of pattern development and the response time scales of the bedforms to changing environmental boundary conditions. Examining multiple spatial scales of bedforms in the context of the formative boundary conditions maximizes environmental reconstructions and provides a means to extract specific wind and sediment supply signals from dune-field patterns.

1.1. Multi-spatial dune-field pattern analysis

The appropriateness of a multi-spatial approach to pattern analysis arises because aeolian dune-field patterns form over a wide range of

* Corresponding author. Tel.: +1 979 845 2089.
E-mail address: rce@tamu.edu (R.C. Ewing).

http://dx.doi.org/10.1016/j.geomorph.2014.11.023
0169-555X/

spatial and temporal scales and in response to environmental boundary conditions that change over wide spatial, temporal and magnitude ranges. Where different scales of bedforms coexist in a dune field, a potentially rich record of pattern forming processes and changing environmental conditions exist.

The coexistence of different spatial scales of bedforms within a dune field can be thought of as occurring within a single type of bedform or between types of bedforms. Within a single type of bedform, patterns emerge through different stages of pattern development by interactions at the fluid-grain, flow-form, and dune–dune scales (Werner, 1999; Kocurek et al., 2010). These different interactions generate distinct bed morphologies, such as dunes, protodunes, lee slope processes and dune defects (Werner, 1999; Murray et al., 2014). These bed morphologies are modified over different time scales, thus creating unique environmental records over a range of time scales. In addition to varying stages of pattern development, distinct types of bedform coexist within a single dune field, such as ripples, coarse-grained ripples and dunes. Different types of bedform arise through different formative mechanisms, respond to environmental changes over different time scales and create unique environmental records (Sharp, 1963; Andreotti et al., 2006; Yizhaq et al., 2012; Murray et al., 2014). Analysis of bedforms at different stages of development and of different types provides a means to recognize environmental changes over different time scales (Fig. 1).

Dune-field pattern boundary conditions, such as sediment supply, availability and wind transport capacity and direction change over a wide range of time scales (Fig. 1). Sediment supply, as the source material for dune fields (e.g. Kocurek and Lancaster, 1999), may be generated instantaneously, as with impact shattering, or over much longer time scales, as with uplift, weathering and erosion of bedrock (see review in Kocurek and Ewing, 2012). Sediment availability within a dune field may change spatially or temporally because of surface moisture, coarse lag, vegetation, binding, cementation, biologic or evaporite crusts (Kocurek and Lancaster, 1999). Changes in the wind transport capacity and direction may occur because of turbulent gusts (Frank and Kocurek, 1994), diurnal winds (Hunter and Richmond, 1988), storm winds (Hunter et al., 1983; Elbelrhiti et al., 2005), katabatic winds (Howard, 2000; Bourke et al., 2009; Ewing et al., 2010), monsoonal winds (Weijian et al., 1996; Loope et al., 2001; Mason et al., 2009), seasonal winds (Hummel and Kocurek, 1984; Kocurek et al., 1992), decadal to centennial wind events (Hugenholtz and Wolfe, 2005; Jewell and Nicoll, 2011; Lancaster and McCarley-Holder, 2013), millennial events (Hanson et al., 2010), and orbital cycles (e.g. tens of thousands of years), such as Milankovitch cycles (Warren and Allison, 1998; Lancaster et al., 2002) (Fig. 1).

The range of winds acting upon a dune field is typically complex despite relatively simple dune-field patterns that may emerge. Analysis of the wind patterns reveals the signal lost by looking at one scale of pattern, implies a rich climate record and motivates the need to for multi-scale pattern analysis. For example, White Sands Dune Field in New Mexico, USA displays a simple crescentic dune pattern that is nearly transverse to the overall wind regime (Fig. 2), but the wind

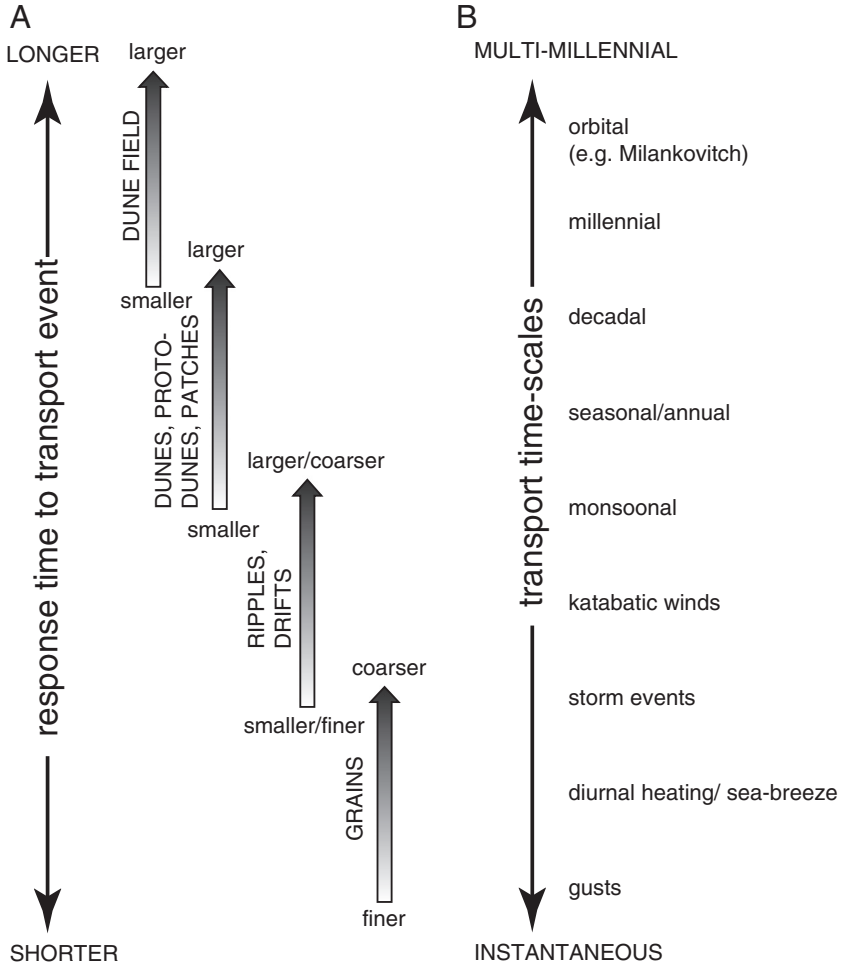

Fig. 1. Schematic showing (A) relative response time scales of different spatial scales of bedforms and (B) different time scales of transport events. Though much overlap occurs in the space and time scales of bedforms and transport events, the range highlights the potential record contained in different bedforms responding over different temporal scales within a single dune field.

Please cite this article as: Ewing, R.C., et al., Multi-spatial analysis of aeolian dune-field patterns, Geomorphology (2014), http://dx.doi.org/10.1016/j.geomorph.2014.11.023

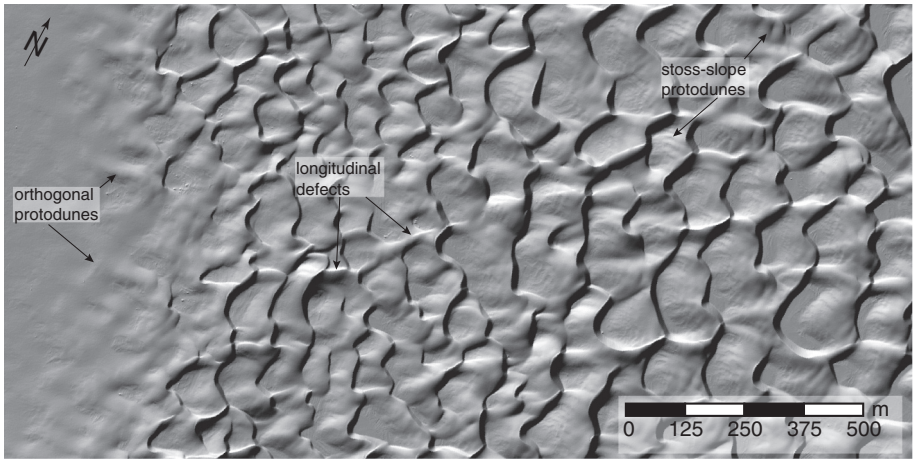

Fig. 2. Shaded relief image of the upwind margin of White Sands Dune Field, New Mexico derived from airborne light detection and ranging (lidar). Primary transport direction is SW–NE. Black arrows and labels highlight morphologic features of the dune field that indicate a complex wind regime. Orthogonal protodunes at the upwind margin are defined by low-relief topography with intersecting crests that emerge prior to the fully developed dunes. Longitudinal defects extend approximately parallel to the primary transport direction and persist downwind for several wavelengths. Stoss-slope protodunes form on the windward slopes of the primary dune and are smaller in scale than the upwind margin protodunes. Lidar from www.opentopography.org.

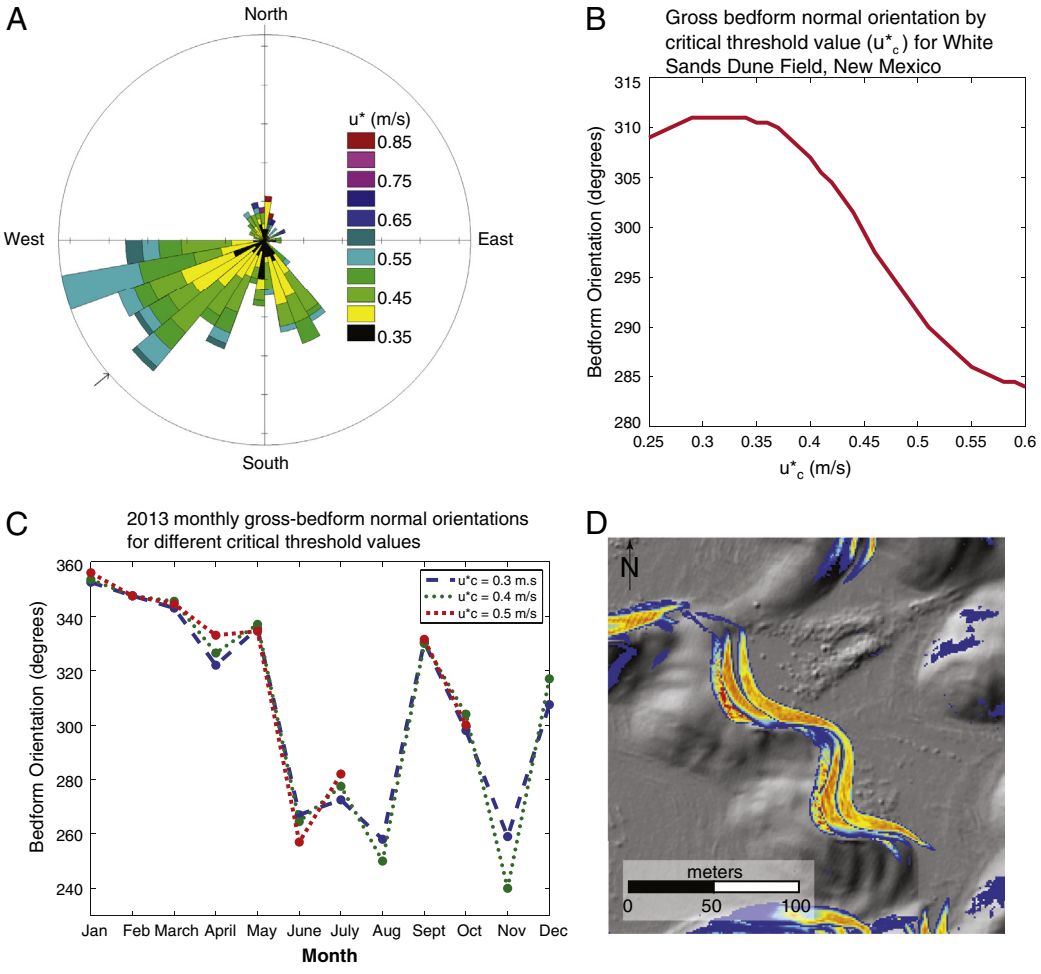

Fig. 3. Components of the complex wind regime at White Sands Dune Field in New Mexico. (A) Wind rose showing the distribution of winds above the critical threshold for sand transport at White Sands Dune Field. The threshold value from Eastwood et al. (2012). Black arrow in SW quadrant of wind rose indicates the resultant transport direction from the SW. (B) Predicted gross-bedform normal orientations for different critical threshold values. Within the range of measured threshold values ~0.25 m/s to 0.35 m/s, the predicted dune orientations fall within the range of those measured by Baitis et al. (2014). Note that bedform orientation could vary where threshold values are higher, such as where moisture or grain size limits the mobilization of grains. (C) Monthly gross bedform normal crestline orientations calculated from the 2013 wind regime at White Sands Dune Field show that bedforms with short reconstitution times may reflect different winds at different times of the year. (D) Oblique migration or 'crabbing' of a crescentic dune at White Sands Dune field. Image shows only lee slope values greater than 20° over three time periods from 2007, 2008 and 2010. Dune migration is from the SW to NE in the image. Slope values are overlain on a shaded relief image derived from airborne lidar.
Lidar from www.opentopography.org.

Please cite this article as: Ewing, R.C., et al., Multi-spatial analysis of aeolian dune-field patterns, Geomorphology (2014), http://dx.doi.org/10.1016/j.geomorph.2014.11.023

distribution is complex with three distinct modes (Fig. 3A). The range of winds can be related to typical westerly winds, storm fronts and monsoonal winds (Jewell and Nicoll, 2011). The predicted dune orientations based on gross-bedform normal transport (Rubin and Hunter, 1987) for a range of critical threshold values are approximately what are measured at White Sands (Fig. 3B). However, a range of other bedform orientations are possible where different critical threshold values are expected (Fig. 3B). Additionally, different bedform orientations would be expected at different times of the year for bedforms that reconstitute (i.e., change orientation) over shorter time scales (Fig. 3C).

Pattern signatures of the complexity of the winds at White Sands Dune Field are the prevalence of crestlines longitudinal to the primary southwesterly wind and orthogonal to the primary NE SW crestline orientation, orthogonal protodunes at the upwind margin and protodunes formed on the stoss slopes of the crescentic dunes (Fig. 2). Multitemporal imagery reveals the oblique migration of the crescentic ridges and implies at least two components of a complex wind regime (Fig. 3D). Additionally, that the oblique component of migration is toward the south suggests that the strongest secondary wind component is likely from the north, which is clear in the wind rose.

2. Multi-spatial analysis within one type of bedform

Field (Kocurek et al., 1992; Ping et al., 2014), laboratory (Rubin and Ikeda, 1990; Reffet et al., 2010) and modeling (Landry and Werner, 1994; Werner, 1995; Bishop et al., 2002; Zhang et al., 2010) efforts, demonstrate that bedform patterns emerge through stages of development, each with a distinct morphologic character and a set of associated processes. These different morphologic and process stages of development provide the basis for multi-spatial analysis within one type of bedform.

The development of aeolian dunes is characterized by a transition from sand patches to proto-dunes to dunes to dune-field patterns (Kocurek et al., 1992; Werner, 1995; Lancaster, 1996; Ping et al., 2014). In dune fields with distinct point or line sources of sediment (e.g. Ewing and Kocurek, 2010) the patch to dune transition occurs spatially across the field from the upwind source area where dune emergence is initiated (Figs. 2 and 4). Thus, the margins of dune fields are an obvious target for analyzing the full range of morphologic stages (Figs. 2 and 4). Early stages of bedforms are not as apparent in well-developed dune fields that emerge from a plane-source of sediment (e.g. Ewing and Kocurek, 2010) because the bedforms develop synchronously across the field (Kocurek et al., 1992; Ping et al., 2014). Protodunes also form by calving from fully-developed dunes, in interdune areas and on the stoss slopes of larger dunes. Beyond the initiation of the first dune, pattern development occurs with changes in dune size, morphology and crestline pattern through pattern coarsening via dune interactions (Landry and Werner, 1994). Given the different spatial scales associated with each morphologic stage of pattern development, each stage is at least potentially a distinct environmental indicator that responds to different time scales of changing conditions.

Process-stages of bedform development occur as fluid-grain, dune-flow and dune-dune interactions (Werner, 1999; Kocurek et al., 2010). Observations of the fluid-grain level of interaction are typically below the spatial and temporal resolution limits of most airborne or satellite remotely sensed data, but dune-flow and dune-dune interactions are readily visible in most imagery. One way in which dune-flow interactions are represented in remote imagery is through recognition of lee slope processes, which vary with wind direction and local crestline orientation (Sweet and Kocurek, 1990; Eastwood et al., 2012) (Fig. 5). Grainflow, grainfall or wind ripple stratification form distinct patterns on the lee slope of dunes and provide a detailed map of how primary and dune-modified winds are affected by the crestline position (Fenton et al., 2003; Ewing et al., 2010; Eastwood et al., 2012). Dune defects, which are the low-volume ends of dunes through which some dune interactions occur, have distinct morphologic character and

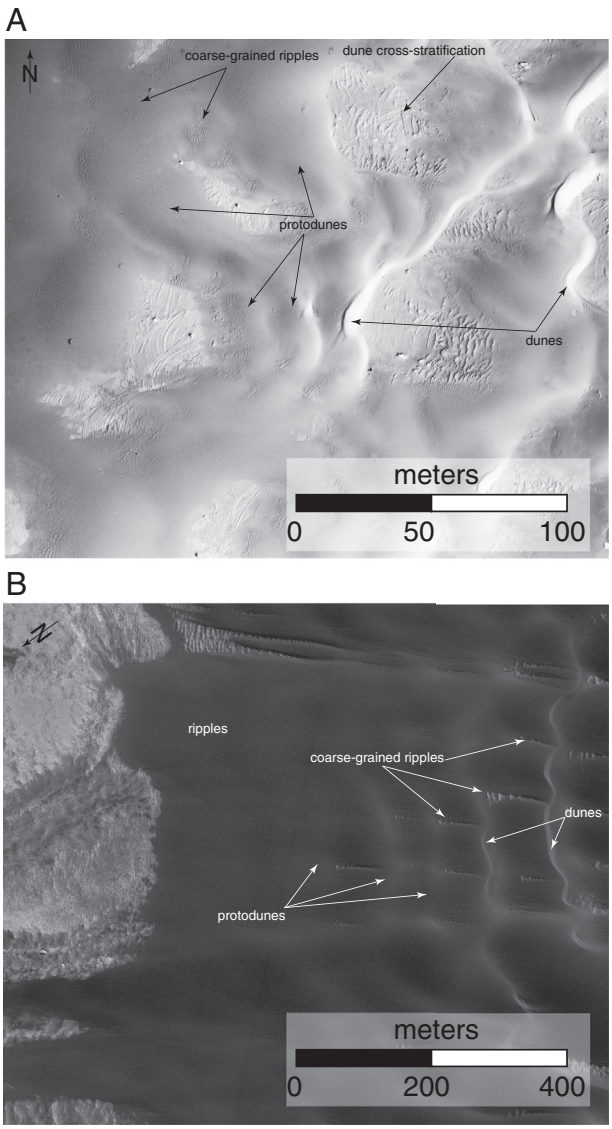

Fig. 4. The upwind margins of (A) White Sands Dune Field, New Mexico, USA and (B) Olympia Undae Dune Field, Mars near Cavi Reentrant adjacent to the permanent north polar ice cap on Mars. In both images, coarse-grained ripples, protodunes and dunes are highlighted by arrows and labels. Wind ripples are below the resolution of the imagery at White Sands Dune field, but apparent in the HiRISE imagery on Mars. Mars image is HiRISE PSP_010097_2650_RED.
White Sands image is an airborne orthophotograph provided by Gary Kocurek.

respond to winds on time scales shorter than dunes (Landry and Werner, 1994; Werner and Kocurek, 1997). Though relatively unexplored, different styles of bedform and defect interactions may indicate details of a wind regime not apparent in the gross dune pattern. Overall, the processes at the fluid-grain, flow-form stages of dune field development provide a higher temporal-resolution environmental signal than the pattern-scale processes, which reflect the integrated signal.

2.1. Examples of patterns across a single type of bedform

2.1.1. Sand patches and protodunes

Sand patches and protodunes are characteristic emergent bedforms created in the early stages of dune development (Kocurek et al., 1992; Werner, 1995; Lancaster, 1996; Momiji et al., 2002; Elbelrhiti et al., 2005) (Fig. 4). Because protodunes are thought to directly relate to fluid-grain and dune-flow interactions (e.g. Andreotti et al., 2010), these bedform types have among the greatest potential for

Please cite this article as: Ewing, R.C., et al., Multi-spatial analysis of aeolian dune-field patterns, Geomorphology (2014), http://dx.doi.org/10.1016/j.geomorph.2014.11.023

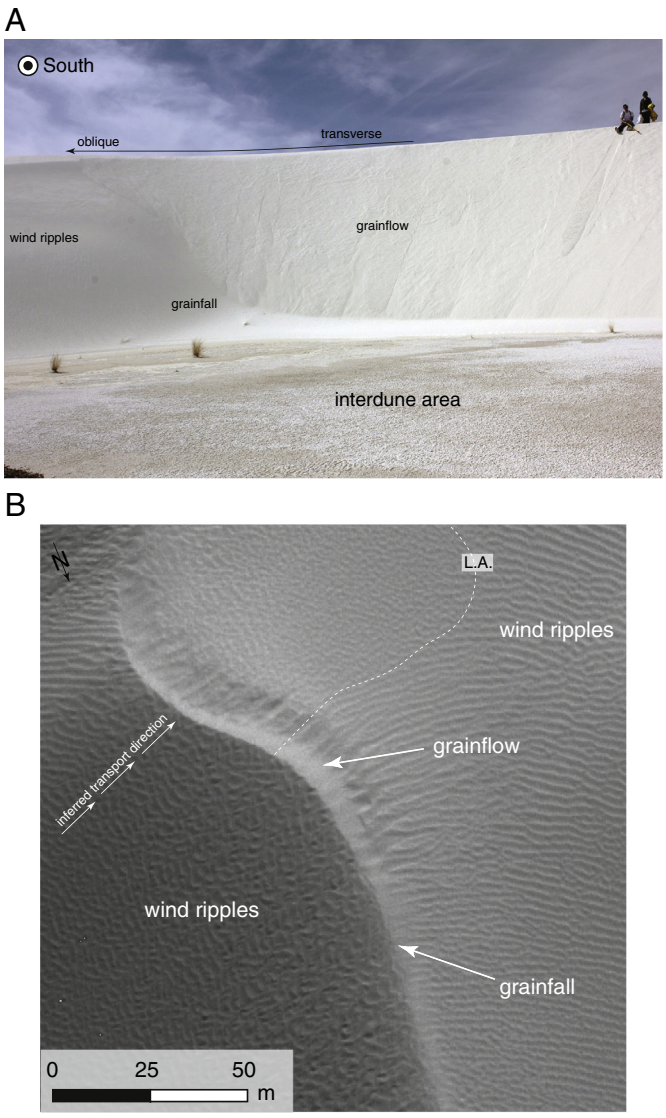

Fig. 5. Images showing changes in dune lee slope stratification determined by an incident angle. (A) Ground image taken at White Sands Dune Field of the lee slope of a dune toward the south. The different types of stratification are labeled and change laterally from the right to the left in the image as the curvature of the brinkline changes. People on the brinkline in the upper right of the image for scale. (B) HiRISE image PSP_001432_2610 in Olympia Undae Dune Field showing variations in lee slope stratification type by an incident angle (e.g. Ewing et al., 2010). Stratification changes from grainfall and wind ripples to grainflow dominated lee slope as the curvature of the crestline changes. Wind ripples superimposed on the stoss-slope show transverse flows at the dune brink where the lee slope is grainflow dominated. Also note the mottled ripple texture in the interdune area delineated by the line of attachment (L.A.) that indicates the low-velocity recirculation cell in the lee of the transverse areas of the dune.

understanding grain size, density and atmospheric density in dune fields from remote sensing data. However, our understanding of how fluid-grain dynamics relate to protodune morphology and the role of protodunes in overall dune-field pattern formation is in its infancy (Andreotti et al., 2010; Claudin et al., 2013). In one iteration, for example, protodune wavelength is thought to scale with drag length, which relates to the submerged sediment density ($\rho s/\rho f$) and grain diameter (Claudin and Andreotti, 2006). Where measured on the Earth, this relationship approximates protodune wavelengths over an erodible substrate for a number of types of bedform (Elbelrhiti et al., 2005; Andreotti et al., 2010). For example, at the White Sands Dune Field, New Mexico (Figs. 2 and 4A) the grain size at the upwind margin is around 0.5 mm and composed of gypsum, which has a density of 2.312 g/cm (Jerolmack et al., 2011). These parameters predict a protodune wavelength of around 50 m, which is on the order of what can be measured from aerial imagery and digital terrain models, though a wide range of wavelengths are visible (Fig. 4A). On Mars, however, the relationship appears to break down. Protodune wavelength of around 400–600 m are predicted by numerical models and empirical relationships on Earth (Claudin and Andreotti, 2006), but protodunes on Mars appear to emerge at wavelengths around Earth values (Fig. 4B). The response of protodunes to differing wind directions is not well understood, but protodunes with orthogonally intersecting crestlines are observed at the White Sands Dune Field (Fig. 2). The pattern of protodune crestlines is different from the dominant dune crestline pattern within the White Sands Dune Field. This may relate to the overall complicated wind regime at White Sands, where smaller bedforms with shorter reconstitution times would be expected to be oriented differently throughout the year (Fig. 3). Similar variability in protodune orientation associated with complicated wind regimes has been reported in Ping et al. (2014).

2.1.2. Lee slope processes

Lee slope processes have been widely used in determining wind flow patterns in dune fields from remote imagery (Fenton et al., 2003; Ewing et al., 2010; Gardin et al., 2012; Silvestro et al., 2013). Most methodologies infer that, in transverse wind regimes, the steepest, grainflow-dominated slopes form nearly orthogonal to geologically recent dominant winds. However, lee-slope stratification type is remarkably sensitive to incident angle (Sweet and Kocurek, 1990), which is the angle between wind and the dune brinkline. A high spatial resolution record of winds can be extracted through the analysis of types of lee slope stratification. Eastwood et al. (2012) elucidate permutations of the relationships between wind direction, brinkline orientation, dune sinuosity and wind speed, but the results can be summarized as grainfall/grainflow occurs where the incident angle is between 70–90°, grainfall/grainflow with wind-rippled bottom sets occur at 40–70°, wind ripples occur at 25–40°, erosional surfaces occur at angles up to 15° and bypass surfaces up to 25°. Using High Resolution Imaging Science Experiment (HiRISE) imagery (McEwen et al., 2007), this methodology was employed in the Olympia Undae Sand Sea in the North Polar Region of Mars to show how the interplay of two winds create a complex (i.e., multigenerational) pattern (Ewing et al., 2010). Digital terrain models, which are now widely available for dune fields on Mars, offer an additional level of analysis where aspect and slope can be related to potential wind directions (Silvestro et al., 2013).

3. Multi-spatial analysis across types of bedform

The intersection of spatial scales of bedforms is most clearly represented by the superposition of different bedform types in a single dune field. Ripples, coarse-grained ripples and dunes typically occur collocated within a single dune field. These bedform types reflect different formative mechanisms and spatially and temporally distinct boundary conditions. The intersection of different types of bedforms are useful for environmental reconstructions because the interactions between these types of bedforms are relatable in terms of relative grain size and transport rates. Spatial grain sorting across a dune field gives rise to distinct bedform types such as coarse-grained ripples, which can be distinguished based upon the morphologic characteristics from typical wind ripples. Differences in spatial scales between dunes, ripples and coarse-grained ripples provide a means to infer relative response times to the wind. Smaller, faster migrating bedforms will reconstitute over shorter time scales than larger, slower migrating time scales (Rubin and Ikeda, 1990; Werner and Kocurek, 1997; Chojnacki et al., 2014) and, thus, to respond to shorter duration wind events.

Please cite this article as: Ewing, R.C., et al., Multi-spatial analysis of aeolian dune-field patterns, Geomorphology (2014), http://dx.doi.org/10.1016/j.geomorph.2014.11.023

3.1. Examples of patterns across a types of bedform

3.1.1. Intersection of ripples and dunes

The juxtaposition of ripple and dune patterns reflects two related time scales of transport because both are forming simultaneously under the same overall wind regime, yet respond to different components of the wind regime. Ripples are ubiquitous across dune fields and are the smallest wind-blown bedforms. Thus, these bedforms respond to short-during transport events. On Earth, ripples formed within the typical 100–300 μm sand size range tend toward the decimeter scale (Sharp, 1963; Landry and Werner, 1994) and typically reorganize during a single wind event. Ripples can fairly reliably be used as indicators of wind direction associated with the most recent transport event if local dune slope is accounted for (Howard, 1977; Kocurek et al., 2007). On Mars, ripples found superimposed upon sand dunes tend to be larger than those on Earth, ranging up to several meters in wavelength (Ewing et al., 2010; Bridges et al., 2012). Martian ripples also likely represent the most recent transport event, but because of their size Martian ripples may integrate winds over several transport events from different directions.

Though ripples migrating over sand dunes have been used to infer transport conditions on Earth (Howard, 1977; Kocurek et al., 2007), mapping ripples on Mars is more common because few other means exist to infer wind direction and ripples are visible in satellite imagery (Ewing et al., 2010; Silvestro et al., 2010; Bridges et al., 2012). On Mars, the ripple–dune relationship has been used to infer directions of recent transport events and stoss and lee secondary flow directions and dynamics (Ewing et al., 2010; Silvestro et al., 2013). Using multi-temporal imagery the juxtaposition of ripples and dunes has been used to infer sand movement, sand fluxes, fractions of reptation and saltation in transport wind speed up over dunes (Silvestro et al., 2010, Bridges et al., 2011, 2012, 2013) (Fig. 6).

Variations in ripple wavelength, orientation and rates of migration provide insights to dune-flow interactions. Ripple wavelength tends to increase with increased wind speed (Seppälä and Lindé, 1978; Andreotti et al., 2006) such that ripples may increase in wavelength up dune topography and reflect the role of stoss slope curvature in wind speed-up over a dune. Multi-temporal data of ripple migration over dunes reveals the wind speed over dune topography by an increase in the rate of ripple migration (Bridges et al., 2012). Ripple orientations also reveal flows deflected by dune topography. Ripples moving up the convex areas of a stoss slope of a dune are deflected laterally to the dune flanks and ripples migrating up concave areas of a stoss slope tend to fan outward toward the crestline (Howard, 1977; Kocurek et al., 2007). Ripple orientation at the brinkline of a dune provides a measure of the wind direction at the brink, thus the incident angle, which can be compared with the types of lee slope stratification.

3.1.2. Intersection of coarse-grained ripples, ripples and dunes

The juxtaposition of ripples with two distinct wavelengths provides a means to recognize two grain-size populations because coarse-grained ripples tend to have greater wavelengths (Sharp, 1963; Seppälä and Lindé, 1978). The presence of ripples and coarse-grained ripples implies a variation in sediment supply (i.e. grain size) and spatial sorting of grains related to proximity to source and secondary wind flow patterns (Jerolmack et al., 2006, 2011). From a given supply of sediment, sand-size fractions segregate over short distances such that the coarsest fraction tends to form coarse-grained ripples or other bedforms like zibars. These types of bedforms are prominent at the upwind margins of dune fields where coarse grains concentrate as a lag as the dune field migrates downwind (Nielson and Kocurek, 1986; Sweet et al., 1988). On the stoss slope of a dune, coarse-grained ripples cluster in low-lying areas such as concavities along the stoss slope or interdune areas because of the slope effects on the threshold for transport (Howard, 1977).

3.1.3. Intersection of dunes and dunes

Complex, multigenerational dunes form two or more distinct populations of pattern parameters such as dune spacing and crestline orientation and form under temporally discrete boundary conditions (Ewing and Kocurek, 2010) (Fig. 7). This type of dune-field pattern is distinct from dunes that host superimposed dunes that are in equilibrium with primary and secondary flows. Complex dunes are recognized indicators of environmental change over long time scales (Lancaster, 1995; Warren and Allison, 1998; Lancaster et al., 2002; Kocurek and Ewing, 2005; Beveridge et al., 2006; Derickson et al., 2008; Grotzinger et al., 2013). Because the superposition of dunes requires the host dune to be large relative to the superimposed dune, the time scales represented to form complex dunes tend to be long. Sufficient constructional time is necessary to form the primary dune and shift in conditions to generate a new superimposed pattern. Time scales for reworking a dune pattern are dependent on wind magnitudes and sediment availability, but for large dunes with slow rates of migration, reorientation times are typically on millennial time scales (Werner and Kocurek, 1997; Ewing et al., 2006).

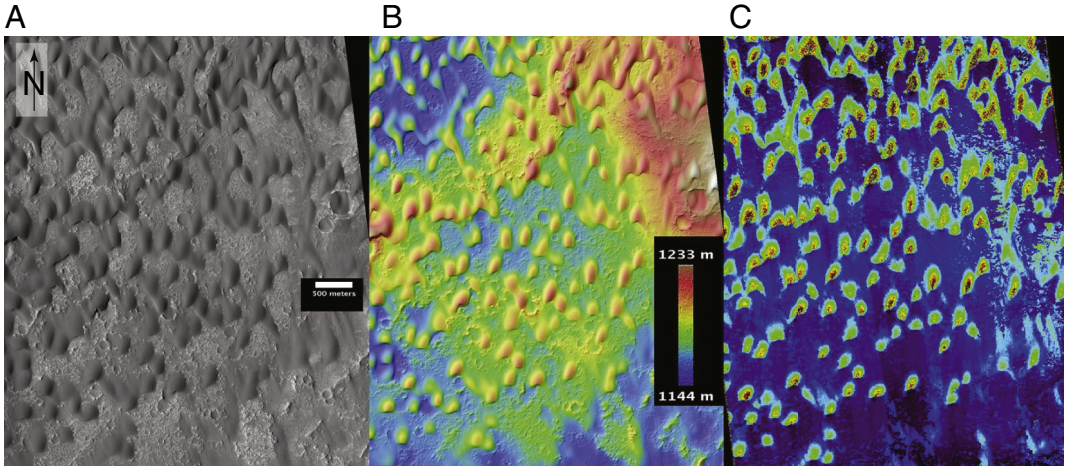

Fig. 6. Sand dunes in Herschel Crater, Mars. (A) HiRISE image showing dune morphology. Transport is from north to south. HiRISE image PSP_003572_1650 (B) HiRISE digital terrain model (DTM) of area shown in (A) HiRISE DTM DTEEC_002860_1650_003572_1650_U01. (C) Displacement map derived from the Cosi-Corr method (Leprince et al., 2007) with HiRISE images to measure displacement of ripples. The reds and browns show higher rates of ripple migration, which occurs at the dune crests and mostly at the upwind area of the dune field. (For interpretation of the references to color in this figure legend, the reader is referred to the web version of this article.)
Images provided by Nathan Bridges and Kirby Runyon.

Please cite this article as: Ewing, R.C., et al., Multi-spatial analysis of aeolian dune-field patterns, Geomorphology (2014), http://dx.doi.org/10.1016/j.geomorph.2014.11.023

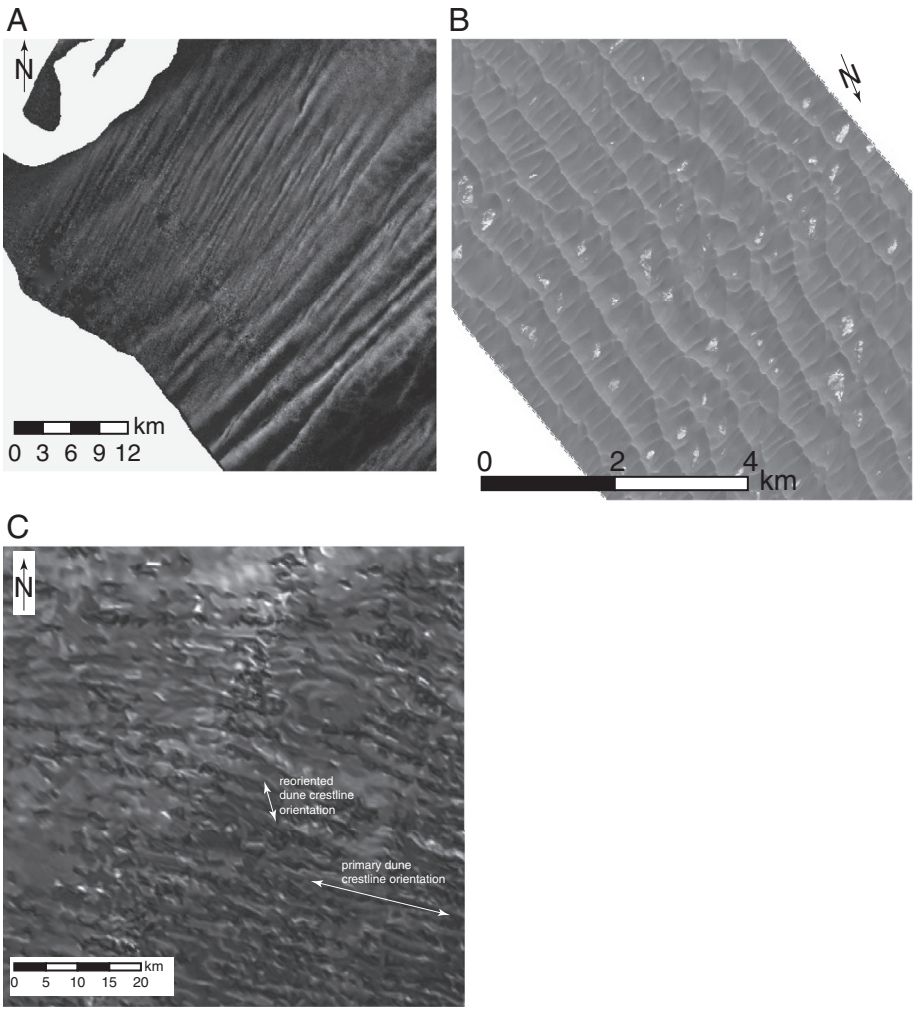

Fig. 7. Superimposed crestlines of different spatial scales and orientations on (A) Earth, (B) Mars and (C) Titan interpreted as complex patterns in which each crestline orientation represents a different generation of dune construction. (A) Shuttle Radar Topography Mission DTM of the Agneitir Sand Sea, Mauritania. (B) HiRISE image PSP_001432_2610 in Olympia Undae Dune Field, Mars. (C) Image from Cassini Synthetic Aperture Radar (SAR) (Elachi et al., 2005) mosaic of Shangri-La Dune Field on Titan at 5.02N, −149.19E showing reoriented dune crestlines superimposed upon larger dunes.
Image provided by Antoine Lucas.

On Earth, Mars and Titan orbital cycles (i.e. tens of thousands of years) affect environmental changes over multi-millennial time scales (DeMenocal et al., 2000; Laskar et al., 2002; Aharonson et al., 2009), which may be reflected in dune-field patterns. For example, along the coastal deserts of Mauritania in western Africa, three generations of dunes, spanning 25,000 years from the Late Glacial Maximum (LGM) to present, were recognized by the superposition of multiple patterns of different scales, orientation and spacing (Fig. 7A) (Lancaster et al., 2002). Stratigraphic observations and optically stimulated luminescence age constraints indicate that the largest patterns formed during the LGM, an intermediate scale pattern formed between 13 and 10 ka and the smallest pattern began to develop around 5 ka (Lancaster et al., 2002). Through a similar approach in the Gran Desierto Sand Sea in Mexico, five generations of patterns were identified (Beveridge et al., 2006) that span a similar time range. Obvious difficulties arise in confirming the presence of a complex pattern where stratigraphic and age constraints are not available.

Complex patterns on Mars have been recognized in the Olympia Undae Dune Field where a reticulate pattern shows the larger pattern being reworked by a smaller pattern (Fig. 7B) (Ewing et al., 2010). This complex pattern is interpreted as a shift in the wind and sediment supply because of the onset of katabatic winds descending from the permanent north polar ice cap of Mars. The change in wind direction and increase in sediment supply overprinted an existing dune pattern, which is interpreted to have formed in polar easterly wind regime. Similarly, on Titan, intersecting crestlines of different scales indicate that the largest dunes are being reworked by a younger generation of dunes (Fig. 7C). Based on the morphology of the pattern and modeled rates of reorientation of the largest and smallest scale dunes, this complex pattern is interpreted to have formed from a shift in winds and sediment availability over several thousand Saturn years Ewing et al., (2015).

4. Other wind-related environmental indicators

The scope of this paper focuses on the multiple spatial scales of bedforms found within a dune field because the interplay between these scales contributes to the overall evolution of the dune-field pattern and relative response time scales of the bedforms can be inferred. There are, however, many indicators of winds and sediment transport visible in remote and surface images that have been shown to be useful environmental indicators of sediment transport such as dune cross-stratification (Grotzinger et al., 2005; Ewing et al., 2010; Milliken et al., 2014), ventifacts (Bridges et al., 1999), yardangs (Sefton-Nash et al., 2014), sand shadows (Blake et al., 2013), wind streaks (Howard, 2000), periodic bedrock ridges (Montgomery et al., 2012) and

Please cite this article as: Ewing, R.C., et al., Multi-spatial analysis of aeolian dune-field patterns, Geomorphology (2014), http://dx.doi.org/10.1016/j.geomorph.2014.11.023

transverse aeolian ridges (TARs) (Balme et al., 2008). Difficulties in using these to infer specific components of wind regime arise because the time scales associated with the formation or modification of these features relative to each other or another feature are difficult to constrain from remote images. This may be in part because the physical processes that control the morphologies are poorly understood, such as in TARs for example. Despite some limitations, studies that employ all wind related features tend to have among the most complete environmental reconstructions (Fenton et al., 2003; Silvestro et al., 2011, 2013, Sefton-Nash et al., 2014).

5. Conclusions

The wide spatial and temporal ranges over which aeolian bedforms develop are limiting and fruitful for extracting environmental signals from dune-field patterns. Over the longest time scales and at the largest spatial scales, dune fields integrate wind and sediment supply signals that vary over long-term climate changes. Over the shortest time scales, the smallest bedform patterns may reflect the most recent wind and sediment supply conditions. Analysis of any single scale of bedform can only yield environmental signals associated with the response time of that bedform.

The proposal here, which has been demonstrated by a number of studies, is that multi-spatial analysis of dune-field patterns at a wide range of spatial scales overcomes some of the limitations of observations made only at a single scale of interest. Different scales of bedforms and processes operating in a dune field can be broken into those that are within a single type of bedform and those that occur between different types of bedforms. The latter has yielded the most promising results where mapping ripples on Mars has highlighted a number of important dune-flow related processes and the intersection of dunes of different scales and orientations has yielded interpretations of multiple climatic events (Lancaster et al., 2002; Beveridge et al., 2006; Derickson et al., 2008; Silvestro et al., 2010; Bridges et al., 2012; Ewing et al., 2014).

Future research is dictated by a need for a greater quantitative understanding of how fluid–grain, dune-flow and dune–dune interactions are morphologically expressed. In turn, more research is needed that exploits the existing multi-spatial characteristics of dune fields on other worlds from a process-based perspective. Understanding morphologic relationships between protodunes and fluid–grain/dune-flow interactions is a promising avenue for constraining what are currently among the most critical, but least constrained parameters for dune fields on Mars — grain size, sediment density and to some extent local variations in air density. Understanding protodune dynamics may also elucidate time scales associated with dune formation that could yield better temporal constraints for the overall dune-field pattern formation. Additionally, our current bias is toward understanding pattern dynamics formed on erodible substrates; however, clear dynamical differences exist in the emergence and behavior of dunes on erodible (e.g. sand) and non-erodible substrates (e.g. bedrock) (Courrech du Pont et al., 2014). Laboratory, field and modeling works are needed to understand the range interactions that are distinct in availability-limited dune fields and which may be useful for extracting environmental information.

Continued collection of multi-temporal topographic and high-resolution imagery is needed on Earth and Mars, and ultimately needed for Titan. Techniques, such as optical cross-correlation of HiRISE images as has been done successfully by Bridges et al. (2013), is among the most promising method for characterizing high spatial and temporal resolution sand transports on Mars. Multi-temporal imagery highlights a number of fundamental processes at the fluid–grain and dune-flow interaction levels that would not otherwise be accessible. Multi-temporal imagery provides insights for Mars, specifically the quantification of stoss and lee slope dynamics and field-wide fluxes by a method to better constrain dune dynamics. Noteworthy, is that this type of data is not available on Earth at such high spatial resolutions because of the small scale of the ripples. High spatial and temporal resolution dune-field pattern analyses with mesoscale climate modeling and large eddy simulations are among the most promising methods for understanding flow dynamics related to complex dune-field patterns on Earth, Mars and Titan (Silvestro et al., 2013; Anderson and Chamecki, 2014; Ayoub et al., 2014).

Acknowledgments

This research was supported by NASA through the Cassini Data Analysis Program with a grant 13-CDAPS13_2-0052 to R.C.E. and A.G.H.

References

Aharonson, O., Hayes, A.G., Lunine, J.I., Lorenz, R.D., Allison, M.D., Elachi, C., 2009. An asymmetric distribution of lakes on Titan as a possible consequence of orbital forcing. Nat. Geosci. 2, 851–854. http://dx.doi.org/10.1038/ngeo698.

Anderson, W., Chamecki, M., 2014. Numerical study of turbulent flow over complex aeolian dune fields: the White Sands National Monument. Phys. Rev. E. 89, 013005. http://dx.doi.org/10.1103/PhysRevE.89.013005.

Andreotti, B., Claudin, P., Pouliquen, O., 2006. Aeolian sand ripples: experimental study of fully developed states. Phys. Rev. Lett. 96, 028001. http://dx.doi.org/10.1103/PhysRevLett.96.028001.

Andreotti, B., Claudin, P., Pouliquen, O., 2010. Geomorphology measurements of the aeolian sand transport saturation length. Geomorphology 123, 343–348. http://dx.doi.org/10.1016/j.geomorph.2010.08.002.

Ayoub, F., Avouac, J.-P., Newman, C.E., Richardson, M.I., Lucas, A., Leprince, S., Bridges, N.T., 2014. Threshold for sand mobility on Mars calibrated from seasonal variations of sand flux. Nat. Commun. 5, 5096. http://dx.doi.org/10.1038/ncomms6096.

Baitis, E., Kocurek, G., Smith, V., Mohrig, D., Ewing, R.C., Peyret, A.-P.B., 2014. Definition and origin of the dune-field pattern at White Sands, New Mexico. Aeolian Res. 15, 269–287. http://dx.doi.org/10.1016/j.aeolia.2014.06.004.

Balme, M., Berman, D.C., Bourke, M.C., Zimbelman, J.R., 2008. Transverse aeolian ridges (TARs) on Mars. Geomorphology 101, 703–720. http://dx.doi.org/10.1016/j.geomorph.2008.03.011.

Beveridge, C., Kocurek, G., Ewing, R.C., Lancaster, N., Morthekai, P., Singhvi, A.K., Mahan, S.A., 2006. Development of spatially diverse and complex dune-field patterns: Gran Desierto Dune Field, Sonora, Mexico. Sedimentology 53, 1391–1409. http://dx.doi.org/10.1111/j.1365-3091.2006.00814.x.

Bishop, S.R., Momiji, H., Carretero-González, R., Warren, A., 2002. Modelling desert dune fields based on discrete dynamics. Discret. Dyn. Nat. Soc. 7, 7–17. http://dx.doi.org/10.1080/10260220290013462.

Blake, D.F., Morris, R.V., Kocurek, G., Morrison, S.M., Downs, R.T., Bish, D., Ming, D.W., Edgett, K.S., Rubin, D., Goetz, W., Madsen, M.B., Sullivan, R., Gellert, R., Campbell, I., Treiman, A.H., McLennan, S.M., Yen, A.S., Grotzinger, J., Vaniman, D.T., Chipera, S.J., Achilles, C.N., Rampe, E.B., Sumner, D., Meslin, P.-Y., Maurice, S., Forni, O., Gasnault, O., Fisk, M., Schmidt, M., Mahaffy, P., Leshin, L.A., Glavin, D., Steele, A., Freissinet, C., Navarro-González, R., Yingst, R.A., Kah, L.C., Bridges, N., Lewis, K.W., Bristow, T.F., Farmer, J.D., Crisp, J.A., Stolper, E.M., Des Marais, D.J., Sarrazin, P., 2013. Curiosity at Gale crater, Mars: characterization and analysis of the Rocknest sand shadow. Science 341, 1239505. http://dx.doi.org/10.1126/science.1239505.

Bourke, M.C., Ewing, R.C., Finnegan, D., McGowan, H.A., 2009. Sand dune movement in the Victoria Valley, Antarctica. Geomorphology 109, 148–160. http://dx.doi.org/10.1016/j.geomorph.2009.02.028.

Bridges, N.T., Greeley, R., Haldemann, A.F.C., Herkenhoff, K.E., Kraft, M., Parker, T.J., Ward, A.W., 1999. Ventifacts at the Pathfinder landing site. J. Geophys. Res. 104, 8595. http://dx.doi.org/10.1029/98JE02550.

Bridges, N.T., Bourke, M.C., Geissler, P.E., Banks, M.E., Colon, C., Diniega, S., Golombek, M.P., Hansen, C.J., Mattson, S., McEwen, A.S., Mellon, M.T., Stantzos, N., Thomson, B.J., 2011. Planet-wide sand motion on Mars. Geology 40, 31–34. http://dx.doi.org/10.1130/G32373.1.

Bridges, N.T., Ayoub, F., Avouac, J.-P., Leprince, S., Lucas, a, Mattson, S., 2012. Earth-like sand fluxes on Mars. Nature 485, 339–342. http://dx.doi.org/10.1038/nature11022.

Bridges, N., Geissler, P., Silvestro, S., Banks, M., 2013. Bedform migration on Mars: current results and future plans. Aeolian Res. 9, 133–151. http://dx.doi.org/10.1016/j.aeolia.2013.02.004.

Bullard, J.E., White, K., Livingstone, I., 2011. Morphometric analysis of aeolian bedforms in the Namib Sand Sea using ASTER data. Earth Surf. Process. Landf. 36, 1534–1549. http://dx.doi.org/10.1002/esp.2189.

Chojnacki, M., Johnson, J.R., Moersch, J.E., Fenton, L.K., Michaels, T.I., Bell, J.F., 2014. Persistent aeolian activity at Endeavour crater, Meridiani Planum, Mars; new observations from orbit and the surface. Icarus http://dx.doi.org/10.1016/j.icarus.2014.04.044.

Claudin, P., Andreotti, B., 2006. A scaling law for aeolian dunes on Mars, Venus, Earth, and for subaqueous ripples. Earth Planet. Sci. Lett. 252, 30–44. http://dx.doi.org/10.1016/j.epsl.2006.09.004.

Claudin, P., Wiggs, G.F.S., Andreotti, B., 2013. Field evidence for the upwind velocity shift at the crest of low dunes. Bound.-Layer Meteorol. 148, 195–206. http://dx.doi.org/10.1007/s10546-013-9804-3.

Courrech du Pont, S., Narteau, C., Gao, X., 2014. Two modes for dune orientation. Geology 42, 743–746. http://dx.doi.org/10.1130/G35657.1.

DeMenocal, P., Ortiz, J., Guilderson, T., Adkins, J., Sarnthein, M., Baker, L., Yarusinsky, M., 2000. Abrupt onset and termination of the African Humid Period: rapid climate responses to gradual insolation forcing. Quat. Sci. Rev. 19, 347–361.

Please cite this article as: Ewing, R.C., et al., Multi-spatial analysis of aeolian dune-field patterns, Geomorphology (2014), http://dx.doi.org/10.1016/j.geomorph.2014.11.023

Derickson, D., Kocurek, G., Ewing, R.C., Bristow, C., 2008. Origin of a complex and spatially diverse dune-field pattern, Algodones, southeastern California. Geomorphology 99, 186–204. http://dx.doi.org/10.1016/j.geomorph.2007.10.016.

Eastwood, E.N., Kocurek, G., Mohrig, D., Swanson, T., 2012. Methodology for reconstructing wind direction, wind speed and duration of wind events from aeolian cross-strata. J. Geophys. Res. 117. http://dx.doi.org/10.1029/2012JF002368 (F03035).

Elachi, C., Wall, S., Allison, M., Anderson, Y., Boehmer, R., Callahan, P., Encrenaz, P., Flamini, E., Franceschetti, G., Gim, Y., Hamilton, G., Hensley, S., Janssen, M., Johnson, W., Kelleher, K., Kirk, R., Lopes, R., Lorenz, R., Lunine, J., Muhleman, D., Ostro, S., Paganelli, F., Picardi, G., Posa, F., Roth, L., Seu, R., Shaffer, S., Soderblom, L., Stiles, B., Stofan, E., Vetrella, S., West, R., Wood, C., Wye, L., Zebker, H., 2005. Cassini radar views the surface of Titan. Science 308, 970–974. http://dx.doi.org/10.1126/science.1109919.

Elbelrhiti, H., Claudin, P., Andreotti, B., 2005. Field evidence for surface-wave-induced instability of sand dunes. Nature 437, 720–723. http://dx.doi.org/10.1038/nature04058.

Ewing, R.C., Kocurek, G., 2010. Aeolian dune-field pattern boundary conditions. Geomorphology 114, 175–187. http://dx.doi.org/10.1016/j.geomorph.2009.06.015.

Ewing, R.C., Kocurek, G., Lake, L.W., 2006. Pattern analysis of dune-field parameters. Earth Surf. Process. Landf. 31, 1176–1191. http://dx.doi.org/10.1002/esp.1312.

Ewing, R.C., Peyret, A.P.B., Kocurek, G., Bourke, M., 2010. Dune field pattern formation and recent transporting winds in the Olympia Undae Dune Field, north polar region of Mars. J. Geophys. Res. Planets 115, 1–25. http://dx.doi.org/10.1029/2009JE003526.

Ewing, R.C., Hayes, A.G., Lucas, A., 2015. Sand dune patterns on Titan controlled by long-term climate cycles. Nature Geoscience 8 (1), 15–19. http://dx.doi.org/10.1038/ngeo2323.

Fenton, L.K., Bandfield, J.L., Ward, A.W., 2003. Aeolian processes in Proctor Crater on Mars: sedimentary history as analyzed from multiple data sets. J. Geophys. Res. Planets 108, 1–39. http://dx.doi.org/10.1029/2002JE002015.

Frank, A.J., Kocurek, G.A., 1994. Effects of atmospheric conditions on wind profiles and aeolian sand tranport with an example from White Sands National Monument. Earth Surf. Process. Landf. 19, 735–745.

Gardin, E., Allemand, P., Quantin, C., Silvestro, S., Delacourt, C., 2012. Dune fields on Mars: recorders of a climate change? Planet. Space Sci. 60, 314–321. http://dx.doi.org/10.1016/j.pss.2011.10.004.

Greeley, R., Iversen, J.D., 1985. Wind as a Geological Process on Earth, Mars, Venus and Titan. Cambridge University Press, London.

Grotzinger, J.P., Arvidson, R.E., Bell, J.F., Calvin, W., Clark, B.C., Fike, D.A., Golombek, M., Greeley, R., Haldemann, a., Herkenhoff, K.E., Jolliff, B.L., Knoll, A.H., Malin, M., McLennan, S.M., Parker, T., Soderblom, L., Sohl-Dickstein, J.N., Squyres, S.W., Tosca, N.J., Watters, W.A., 2005. Stratigraphy and sedimentology of a dry to wet eolian depositional system, Burns Formation, Meridiani Planum, Mars. Earth Planet. Sci. Lett. 240, 11–72. http://dx.doi.org/10.1016/j.epsl.2005.09.039.

Grotzinger, J.P., Hayes, A.G., Lamb, M.P., McLennan, S.M., 2013. Sedimentary processes on Earth, Mars, Titan and Venus. In: Mackwell, S.J., Simon-Miller, A.A., Harder, J.W., Bullock, M.A. (Eds.), Comparative Climatoogy of Terrestrial Planets, pp. 439–472 (Tuscon).

Hanson, P.R., Arbogast, A.F., Johnson, W.C., Joeckel, R.M., Young, A.R., 2010. Megadroughts and late Holocene dune activation at the eastern margin of the Great Plains, north-central Kansas, USA. Aeolian Res. 1, 101–110. http://dx.doi.org/10.1016/j.aeolia.2009.10.002.

Howard, A.D., 1977. Effect of slope on the threshold of motion and its application to orientation of wind ripples. Geol. Soc. Am. Bull. 88, 853–856.

Howard, A., 2000. The role of eolian processes in forming surface features of the Martian polar layered deposits. Icarus 144, 267–288. http://dx.doi.org/10.1006/icar.1999.6305.

Hugenholtz, C.H., Wolfe, S.A., 2005. Recent stabilization of active sand dunes on the Canadian prairies and relation to recent climate variations. Geomorphology 68, 131–147. http://dx.doi.org/10.1016/j.geomorph.2004.04.009.

Hummel, G., Kocurek, G., 1984. Interdune areas of the back-island dune field, North Padre Island, Texas. Sediment. Geol. 39, 1–26. http://dx.doi.org/10.1016/0037-0738(84)90022-8.

Hunter, R.E., Richmond, B.M., 1988. Daily cycles in coastal dunes. Sediment. Geol. 55, 43–67. http://dx.doi.org/10.1016/0037-0738(88)90089-9.

Hunter, R., Richmond, B.M., Rho, A.T., 1983. Storm-controlled oblique dunes of the Oregon coast. Geol. Soc. Am. Bull. 94, 1450–1465.

Jerolmack, D.J., Mohrig, D., Grotzinger, J.P., Fike, D.A., Watters, W.A., 2006. Spatial grain size sorting in eolian ripples and estimation of wind conditions on planetary surfaces: application to Meridiani Planum, Mars. J. Geophys. Res. 111, E12S02. http://dx.doi.org/10.1029/2005JE002544.

Jerolmack, D.J., Reitz, M.D., Martin, R.L., 2011. Sorting out abrasion in a gypsum dune field. J. Geophys. Res. — Earth Surf. 116, 1–15. http://dx.doi.org/10.1029/2010JF001821.

Jewell, P.W., Nicoll, K., 2011. Wind regimes and aeolian transport in the Great Basin, U.S.A. Geomorphology 129, 1–13. http://dx.doi.org/10.1016/j.geomorph.2011.01.005.

Kocurek, G., Ewing, R.C., 2005. Aeolian dune field self-organization — implications for the formation of simple versus complex dune-field patterns. Geomorphology 72, 94–105. http://dx.doi.org/10.1016/j.geomorph.2005.05.005.

Kocurek, G., Ewing, R.C., 2012. Source-to-sink: an Earth/Mars comparison of boundary conditions for eolian dune systems. Sediment. Geol. Mars SEPM Spec. Publ. 11, 151–168.

Kocurek, G., Lancaster, N., 1999. Aeolian system sediment state: theory and Mojave Desert Kelso dune field example. Sedimentology 46, 505–515. http://dx.doi.org/10.1046/j.1365-3091.1999.00227.x.

Kocurek, G., Townsley, E.Y., Havholm, K., Sweet, M.L., 1992. Dune and dune-field development on Padre Island, Texas with implications for interdune deposition and water-table controlled accumulation. J. Sediment. Petrol. 62, 622–635.

Kocurek, G., Carr, M., Ewing, R., Havholm, K.G., Nagar, Y.C., Singhvi, A.K., 2007. White Sands Dune Field, New Mexico: age, dune dynamics and recent accumulations. Sediment. Geol. 197, 313–331. http://dx.doi.org/10.1016/j.sedgeo.2006.10.006.

Kocurek, G., Ewing, R.C., Mohrig, D., 2010. State of the Science: how do bedform patterns arise? New views on the role of bedform interactions within a set of boundary conditions. Earth Surf. Process. Landf. 35, 51–63. http://dx.doi.org/10.1002/esp.

Lancaster, N., 1995. Geomorphology of Desert Dunes. Routledge, London.

Lancaster, N., 1996. Field studies of sand patch initiation processes on the northern margin of the Namib Sand Sea. Earth Surf. Process. Landf. 21, 947–954. http://dx.doi.org/10.1002/(SICI)1096-9837(199610)21:10<947::AID-ESP634>3.0.CO;2-7.

Lancaster, N., McCarley-Holder, G., 2013. Decadal-scale evolution of a small dune field: Keeler Dunes, California 1944–2010. Geomorphology 180–181, 281–291. http://dx.doi.org/10.1016/j.geomorph.2012.10.017.

Lancaster, N., Kocurek, G., Singhvi, A., Pandey, V., Deynoux, M., Ghienne, J.-F., Lo, K., 2002. Late Pleistocene and Holocene dune activity and wind regimes in the western Sahara Desert of Mauritania. Geology 991–994.

Landry, W., Werner, B.T., 1994. Computer simulations of self-organized wind ripple patterns. Phys. D 77, 238–260.

Laskar, J., Levrard, B., Mustard, J.F., 2002. Orbital forcing of the Martian polar layered deposits. Nature 419, 375–377. http://dx.doi.org/10.1038/nature01066.

Leprince, S., Ayoub, F., Klinger, Y., Avouac, J.-P., 2007. Co-registration of optically sensed images and correlation (COSI-Corr): an operational methodology for ground deformation measurements. 2007 IEEE International Geoscience and Remote Sensing Symposium. IEEE, pp. 1943–1946 http://dx.doi.org/10.1109/IGARSS.2007.4423207.

Loope, D.B., Rowe, C.M., Joeckel, R.M., 2001. Annual monsoon rains recorded by Jurassic dunes. Nature 412, 64–66. http://dx.doi.org/10.1038/35083554.

Mabbutt, J.A., Wooding, R.A., 1983. Analysis of longitudinal dune patterns in the northwestern Simpson Desert, central Australia. Z. Geomorphol. Supp. 15, 51–69.

Mason, J.A., Lu, H., Zhou, Y., Miao, X., Swinehart, J.B., Liu, Z., Goble, R.J., Yi, S., 2009. Dune mobility and aridity at the desert margin of northern China at a time of peak monsoon strength. Geology 37, 947–950. http://dx.doi.org/10.1130/G30240A.1.

McEwen, A.S., Eliason, E.M., Bergstrom, J.W., Bridges, N.T., Hansen, C.J., Delamere, W.A., Grant, J.A., Gulick, V.C., Herkenhoff, K.E., Keszthelyi, L., Kirk, R.L., Mellon, M.T., Squyres, S.W., Thomas, N., Weitz, C.M., 2007. Mars Reconnaissance Orbiter's high resolution imaging science experiment (HiRISE). J. Geophys. Res. 112, E05S02. http://dx.doi.org/10.1029/2005JE002605.

Milliken, R.E., Ewing, R.C., Fischer, W.W., Hurowitz, J., 2014. Wind-blown sandstones cemented by sulfate and clay minerals in Gale Crater, Mars. Geophys. Res. Lett. 41, 1149–1154. http://dx.doi.org/10.1002/2013GL059097.

Momiji, H., Nishimori, H., Bishop, S.R., 2002. On the shape and migration speed of a protodune. Earth Surf. Process. Landf. 27, 1335–1338. http://dx.doi.org/10.1002/esp.410.

Montgomery, D.R., Bandfield, J.L., Becker, S.K., 2012. Periodic bedrock ridges on Mars. J. Geophys. Res. 117. http://dx.doi.org/10.1029/2011JE003970 (E03005).

Murray, A.B., Goldstein, E.B., Coco, G., 2014. The shape of patterns to come: from initial formation to long-term evolution. Earth Surf. Process. Landf. 39, 62–70. http://dx.doi.org/10.1002/esp.3487.

Nielson, J., Kocurek, G., 1986. Climbing zibars of the Algodones. Sediment. Geol. 48, 1–15. http://dx.doi.org/10.1016/0037-0738(86)90078-3.

Parteli, E.J.R., Durán, O., Tsoar, H., Schwämmle, V., Herrmann, H.J., 2009. Dune formation under bimodal winds. Proc. Natl. Acad. Sci. U. S. A. 106, 22085–22089. http://dx.doi.org/10.1073/pnas.0808646106.

Ping, L., Narteau, C., Dong, Z., Zhang, Z., Courrech du Pont, S., 2014. Emergence of oblique dunes in a landscape-scale experiment. Nat. Geosci. 7, 99–103. http://dx.doi.org/10.1038/ngeo2047.

Reffet, E., Courrech du Pont, S., Hersen, P., Douady, S., 2010. Formation and stability of transverse and longitudinal sand dunes. Geology 38, 491–494. http://dx.doi.org/10.1130/G30894.1.

Rubin, D.M., Hunter, R.E., 1987. Bedform alignment in directionally varying flows. Science 237 (80-), 276–278.

Rubin, D., Ikeda, H., 1990. Flume experiments on the alignment of transverse, oblique, and longitudinal dunes in directionally varying flows. Sedimentology 37, 673–684.

Sefton-Nash, E., Teanby, N.A., Newman, C., Clancy, R.A., Richardson, M.I., 2014. Constraints on Mars' recent equatorial wind regimes from layered deposits and comparison with general circulation model results. Icarus 230, 81–95. http://dx.doi.org/10.1016/j.icarus.2013.11.014.

Seppälä, M., Lindé, K., 1978. Wind tunnel studies of ripple formation. Geogr. Ann. Ser. A. Phys. Geogr. 60, 29–42.

Sharp, R.P., 1963. Wind ripples. J. Geol. 71, 617–636.

Silvestro, S., Fenton, L.K., Vaz, D.A., Bridges, N.T., Ori, G.G., 2010. Ripple migration and dune activity on Mars: evidence for dynamic wind processes. Geophys. Res. Lett. 37, L20203. http://dx.doi.org/10.1029/2010GL044743.

Silvestro, S., Vaz, D.A., Fenton, L.K., Geissler, P.E., 2011. Active aeolian processes on Mars: a regional study in Arabia and Meridiani Terrae. Geophys. Res. Lett. 38. http://dx.doi.org/10.1029/2011GL048955 L20201.

Silvestro, S., Vaz, D.A., Ewing, R.C., Fenton, L.K., Rossi, A.P., Michaels, T.I., Flahaut, J., Geissler, P.E., 2013. Pervasive aeolian activity along Curiosity's traverse in Gale Crater, Mars. Geology 41, 479–482.

Sweet, M.L., Kocurek, G., 1990. An empirical model of aeolian dune lee-face airflow. Sedimentology 37, 1023–1038.

Sweet, M.L., Nielson, J., Havholm, K., Farrelly, J., 1988. Algodones dune field of southeastern California: case history of a migrating modern dune field. Sedimentology 35, 939–952. http://dx.doi.org/10.1111/j.1365-3091.1988.tb01739.x.

Warren, A., Allison, D., 1998. The palaeoenvironmental significance of dune size hierarchies. Palaeogeogr. Palaeoclimatol. Palaeoecol. 137, 289–303. http://dx.doi.org/10.1016/S0031-0182(97)00110-7.

Warren, A., Kay, S., 1987. Dune networks. Geol. Soc. Lond. Spec. Publ. 35, 205–212. http://dx.doi.org/10.1144/GSL.SP.1987.035.01.14.

Weijian, Z., Donahue, D.J., Porter, S.C., Jull, T.A., Xiaoqiang, L., Stuiver, M., Zhisheng, A., Matsumoto, E., Guangrong, D., 1996. Variability of monsoon climate in East Asia at

Please cite this article as: Ewing, R.C., et al., Multi-spatial analysis of aeolian dune-field patterns, Geomorphology (2014), http://dx.doi.org/10.1016/j.geomorph.2014.11.023

the end of the last glaciation. Quat. Res. 46, 219–229. http://dx.doi.org/10.1006/qres.1996.0062.
Werner, B.T., 1995. Eolian dunes: computer simulations and attractor interpretation. Geology 23, 1107–1110.
Werner, B.T., 1999. Complexity in natural landform patterns. Science 284, 102–104. http://dx.doi.org/10.1126/science.284.5411.102.
Werner, B.T., 2003. Modeling landforms as self-organized, hierarchical dynamical systems. Geophys. Monogr. Ser. 135, 133–150.
Werner, B.T., Kocurek, G., 1997. Bed-form dynamics: does the tail wag the dog? Geology 25, 771–774.
Yizhaq, H., Katra, I., Isenberg, O., Tsoar, H., 2012. Evolution of megaripples from a flat bed. Aeolian Res. 6, 1–12. http://dx.doi.org/10.1016/j.aeolia.2012.05.001.
Zhang, D., Narteau, C., Rozier, O., 2010. Morphodynamics of barchan and transverse dunes using a cellular automaton model. J. Geophys. Res. 115. http://dx.doi.org/10.1029/2009JF001620 (F03041).

Please cite this article as: Ewing, R.C., et al., Multi-spatial analysis of aeolian dune-field patterns, Geomorphology (2014), http://dx.doi.org/10.1016/j.geomorph.2014.11.023